

A VIRTUAL CONTROL, MESH-FREE COUPLING METHOD FOR NON-COINCIDENT INTERFACES

PAUL KUBERRY¹, PAVEL BOCHEV¹ AND KARA PETERSON¹

¹ Computational Mathematics
Sandia National Laboratories, MS-1320,
Albuquerque, NM 87185-1320, USA
{pakuber,pbboche,kjpeter}@sandia.gov

Key words: Mesh tying, interface problems, virtual Neumann controls, moving least-squares

Abstract.

We present an optimization approach with two controls for coupling elliptic partial differential equations posed on subdomains sharing an interface that is discretized independently on each subdomain, introducing gaps and overlaps. We use two virtual Neumann controls, one defined on each discrete interface, thereby eliminating the need for a virtual common refinement interface mesh. Global flux conservation is achieved by including the square of the difference of the total flux on each interface in the objective. We use Generalized Moving Least Squares (GMLS) reconstruction to evaluate and compare the subdomain solution and gradients at quadrature points used in the cost functional. The resulting method recovers globally linear solutions and shows optimal L^2 -norm and H^1 -norm convergence.

1 INTRODUCTION

Spatially non-coincident discrete interfaces having gaps and overlaps arise in multiple modeling and simulation scenarios. One example is mesh tying where a complex geometric domain is broken into multiple parts and each part is meshed separately; see, e.g., [4, 11, 1, 10]. Other examples include mortar methods [5, 12] for transmission problems with curved interfaces. The bulk of the existing approaches are based on appropriate extensions of traditional Lagrange multiplier formulations to non-coincident interfaces by designating one of the discrete interfaces as a “master” and enforcing state continuity by suitable projections onto that interface. Design of such methods is often accompanied by theoretical and practical difficulties to ensure stable and accurate discrete formulations.

These difficulties have prompted examination of alternative formulations based on, e.g., least-squares principles [1], or nonstandard Lagrange multipliers [11] defined as traces of Raviart-Thomas elements. A fundamentally different and promising approach for problems with non-coincident interfaces is based on coaching the mesh-tying problem into a constrained optimization problem. Such formulations switch the roles of the coupling

conditions and the subdomain equations and transform the interface problem into a virtual control problem in which the coupling conditions define the objective, the subdomain equations define the constraints, and the interface flux serves as a Neumann control.

Although the intent of the early work on such methods was to obtain non-standard domain decomposition methods for matching subdomain interfaces [7, 6], the optimization approach offers some unique advantages in the context of spatially differing interfaces. In particular, treating the transmission condition as an optimization objective rather than a constraint is better suited for non-coincident interfaces because it involves *minimizing* rather than *eliminating* the state mismatch. While mathematically the latter requires a unique interface to compute the exact difference between the states, the former only depends on a reasonably good estimate of the mismatch.

To the best of our knowledge, the paper [9] is the first application of these ideas for non-coincident interface problems. The method in this paper uses standard C^0 piecewise linear elements, a single Neumann control defined on a virtual common refinement interface and mapped back to each discrete interface in a conservative manner, and linear extension of the subdomain states to compute the state mismatch. The method conserves the global interface flux, is first-order accurate in the H^1 -norm and second-order accurate in the L^2 -norm. However, it does not recover globally linear solutions and construction of a virtual common refinement interface mesh can be complicated in three dimensions.

The paper [2] provides a further development of the optimization mesh tying approach, which addresses some of this drawbacks. In this paper we use two virtual Neumann controls, one defined on each discrete interface, thereby eliminating the need for a virtual common refinement interface mesh. Global flux conservation is achieved by including the square of the difference of the total flux on each interface in the objective. The resulting method provably recovers globally linear solutions and shows optimal H^1 -norm convergence. However, the L^2 -norm rate is suboptimal.

The culprit is the inclusion of terms comprising the mismatch between the finite element flux on one of the discrete interfaces and the extension of the flux from the other interface. These terms were required to obtain a well-posed optimization problem. However, because the virtual control on each interface provides a Neumann condition for the respective subdomain problem, optimization forces the control and the finite element flux to be as close as possible. This creates an accuracy bottleneck, as the finite element flux is only first-order accurate.

Removal of this bottleneck requires a more accurate approximation of the discrete flux on each interface. One option is to use variational flux recovery techniques; see, e.g., [3] and [8]. However, using these approaches in our formulation would require assembly of a consistent interface mass matrix and application of its inverse in the objective functional. Because the inverse mass matrix is dense, the latter would have to be performed iteratively, potentially rising the computational cost of the scheme. In addition, the recovered flux would still have to be transferred to the other interface in a way that does not diminish its accuracy.

In this paper we consider a mesh-free alternative, which uses Generalized Moving Least-Squares (GMLS) [13] to reconstruct high-order flux approximation and perform the nec-

essary data transfers between the interfaces. This offers several valuable advantages in the context of non-coincident interfaces. By treating finite element degrees as scattered data sites, the reconstruction process does not require any information about the underlying mesh structure and/or finite element basis functions, and the reconstruction point is not constrained to be in an element. Because GMLS allows approximation of any linear functional from this data, we can combine the gradient reconstruction step with the data transfer step in one single operation requiring the solution of a small, local weighted least-squares problem. Since these problems are independently defined their solution can be performed in parallel.

2 Notation and technical preliminaries

We consider a bounded open region $\Omega \subset \mathbb{R}^d$, $d = 2, 3$ with an interface σ , which splits the domain into non-overlapping subdomains Ω_1 and Ω_2 . Each subdomain is independently partitioned into finite elements \mathbf{k}_i^n comprising conforming finite element meshes Ω_i^h , $i = 1, 2$. We assume that the meshes are constructed by creating first a polygonal approximation of each subdomain by placing nodes on their Dirichlet boundaries $\Gamma_i = \partial\Omega_i \setminus \sigma$, $i = 1, 2$ and the interface σ .

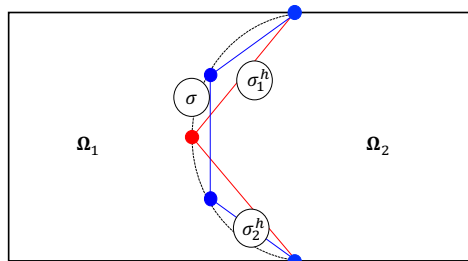


Figure 1: Independent meshing of two subdomains separated by a curved interface σ results in two spatially non-coincident interface grids σ_1^h and σ_2^h .

As a result, each mesh induces a finite element partition σ_i^h , $i = 1, 2$ of σ , containing the element sides \mathbf{s}_i^n that have all their vertices in σ . The resulting interface grids σ_1^h and σ_2^h in general are not spatially coincident and may have gaps and/or overlaps; see Fig. 1.

Given a mesh entity μ we denote the sets of all mesh vertices in μ by $V(\mu)$, e.g., $V(\sigma_i^h)$ are the vertices in the interface mesh σ_i^h and $V(\Omega_i^h)$ is the set of all vertices in the subdomain mesh Ω_i^h .

We denote by $H^1(\Omega_i)$ and $H_{\Gamma_i}^1(\Omega_i)$ the standard Sobolev space of order one on Ω_i , $i = 1, 2$, and its subspace of functions with vanishing trace on Γ_i , respectively. In this paper we restrict attention to piecewise linear, bilinear or trilinear nodal C^0 elements and denote the corresponding conforming finite element subspace of $H^1(\Omega_i^h)$ by H_i^h . We assume that this space is endowed with a Lagrangian basis $\{N_i^k\}$. We will also need the conforming subspace $H_{i,\Gamma}^h$ of $H_{\Gamma_i}^1(\Omega_i^h)$ and the space $H_{i,\sigma}^h$ is spanned by the basis functions associated with vertices on σ_i^h . The traces of the functions in this space form the interface space T_i^h , i.e., $T_i^h = H_{i,\sigma}^h|_{\sigma_i}$. The coefficient vector of $u_i^h \in H_i^h$ is $\mathbf{u}_i \in \mathbb{R}^{n_i}$, where $n_i = |H_i^h|$, the dimension of H_i^h .

2.1 Generalized Moving Least Squares

In this section we briefly review and specialize the GMLS theory to our needs. This theory provides a mesh-free approach to reconstruct the action of a linear functional τ from a scattered set of samples of its argument [13, §4.3].

Here we restrict attention to functionals representing point values of a scalar field or its first derivatives. Specifically, we consider the functionals $\tau_{\mathbf{x}}(u) = u(\mathbf{x})$ and $\tau_{\mathbf{x},i}(u) = \partial_i u(\mathbf{x})$, where $\mathbf{x} \in \mathbb{R}^d$ is the evaluation point. GMLS allows to construct approximations $\tau_{\mathbf{x}}^h$ and $\tau_{\mathbf{x},i}^h$ of these functionals from point samples $\mathbf{u} = \{u(\mathbf{x}_i)\}_{i=1}^N$ contained in a suitable neighborhood of \mathbf{x} and such that $\tau_{\mathbf{x}}^h$ and $\tau_{\mathbf{x},i}^h$ are exact for all $p \in P_m$, where P_m is the space of all multivariate polynomials of degree less than or equal to m with basis $\mathbf{p} = \{p_i\}_{i=1}^Q$. Selection of the data sites is accomplished by a smooth “window” function $\omega(\mathbf{x}, \mathbf{y})$ whose support is contained in a ball of radius ϵ . The size of this ball depends on the polynomial degree m and the density of the data sites \mathbf{x}_i .

One can show that the GMLS approximations of these functionals are given by

$$\tau_{\mathbf{x}}^h(u) = \sum_{k=1}^Q c_k(\mathbf{u}, \mathbf{x}) \tau_{\mathbf{x}}(p_k) = \mathbf{c}^\top(\mathbf{u}, \mathbf{x}) \mathbf{p}(\mathbf{x}), \quad (1)$$

and

$$\tau_{\mathbf{x},i}^h(u) = \sum_{k=1}^Q c_k(\mathbf{u}, \mathbf{x}) \tau_{\mathbf{x},i}(p_k) = \mathbf{c}^\top(\mathbf{u}, \mathbf{x}) \partial_i \mathbf{p}(\mathbf{x}), \quad (2)$$

respectively, where the coefficients $\mathbf{c}^\top(\mathbf{u}, \mathbf{x})$ solve the following weighted least-squares problem:

$$\mathbf{c}(\mathbf{u}, \mathbf{x}) = \underset{\mathbf{b} \in \mathbb{R}^Q}{\operatorname{argmin}} \frac{1}{2} (\mathbf{R}\mathbf{b} - \mathbf{u})^\top W(\mathbf{x}) (\mathbf{R}\mathbf{b} - \mathbf{u}). \quad (3)$$

In (3) \mathbf{R} is $N \times Q$ matrix with element $R_{ij} = p_j(\mathbf{x}_i)$ and $W(\mathbf{x})$ is $N \times N$ diagonal matrix: $W(\mathbf{x}) = \operatorname{diag}(\omega(\mathbf{x}, \mathbf{x}_1), \dots, \omega(\mathbf{x}, \mathbf{x}_N))$. It is straightforward to see that

$$\mathbf{c}(\mathbf{u}, \mathbf{x}) = (\mathbf{R}^\top W(\mathbf{x}) \mathbf{R})^{-1} \mathbf{R}^\top W(\mathbf{x}) \mathbf{u}. \quad (4)$$

Note that the GMLS coefficients $\mathbf{c}(\mathbf{u}, \mathbf{x})$ depend on the point \mathbf{x} and on the data sample \mathbf{u} but not on the functional being approximated. As a result, both (1) and (2) use the same set of coefficients $\mathbf{c}(\mathbf{u}, \mathbf{x})$, i.e., the linear system (4) must be solved only once for every point.

In this paper we apply GMLS with $m = 2$, which is sufficient to recover the accuracy of the linear, bilinear or trilinear finite element spaces used to discretize the problem, as well as sufficiently high order to evaluate partial derivatives with second order accuracy. Because we consider general unstructured finite element meshes, we use dynamic window functions that change the size of their support depending on the node density near the evaluation point \mathbf{x} .

3 Model problem

We consider a scalar elliptic interface problem comprising a pair of subdomain equations

$$\begin{cases} -\nabla \cdot (\kappa_i \nabla u_i) &= f_i \quad \text{in } \Omega_i, \quad i=1,2 \\ u_i &= 0 \quad \text{on } \Gamma_i, \quad i=1,2 \end{cases} \quad (5)$$

augmented with a standard set of transmission conditions

$$u_1 = u_2 \quad \text{and} \quad \kappa_1 \nabla u_1 \cdot \mathbf{n} = \kappa_2 \nabla u_2 \cdot \mathbf{n} \quad \text{on } \sigma. \quad (6)$$

In (5)–(6), \mathbf{n} is a unit normal¹ on σ and κ_i is a positive constant on Ω_i .

Following [2] the starting point for our new method is the following optimization problem:

$$\text{minimize } J_\delta(u_1, u_2, g_1, g_2) \text{ over } H_{\Gamma_1}^1(\Omega_1) \times H_{\Gamma_2}^1(\Omega_2) \times L^2(\sigma) \text{ subject to (8),} \quad (7)$$

where the constraints are given by the variational equations *seek* $u_i \in H_{\Gamma_i}^1(\Omega_i)$ *such that*

$$\kappa_i(\nabla u_i, \nabla v_i)_{\Omega_i} = (f_i, v_i)_{\Omega_i} + \langle g_i, v_i \rangle_\sigma \quad \forall v_i \in H_{\Gamma_i}^1(\Omega_i), \quad i = 1, 2; \quad (8)$$

and the objective is defined as

$$J_\delta(u_1, u_2, g_1, g_2) = \frac{1}{2} \left[\int_\sigma (u_1 - u_2)^2 dS + \int_\sigma ((\kappa_1 \nabla u_1 - \kappa_2 \nabla u_2) \cdot \mathbf{n})^2 dS \right. \\ \left. + \left(\int_\sigma g_1 dS + \int_\sigma g_2 dS \right)^2 + \delta_1 \int_\sigma g_1^2 dS + \delta_2 \int_\sigma g_2^2 dS \right] \quad (9)$$

Formally, the objective (9) is defined only for a single interface σ . However, the structure of J_δ is such that it can be easily extended to the case of non-coincident discrete interfaces σ_1^h and σ_2^h . Indeed, the first two terms measure the mismatches between the states and their interface fluxes. Because (7) aims to minimize rather than to eliminate these mismatches, these terms can be replaced by pairs of terms on σ_1^h and σ_2^h , respectively, measuring the mismatches between the fields and fluxes on each respective interface and an appropriate reconstruction of these quantities from the other interface. Thanks to the use of two independent control variables the last group of terms also admits a straightforward extension: we simply assign control g_i to interface σ_i^h .

To carry out this agenda we need the following operators and spaces:

- A state reconstruction operator R_i , which approximates the values of u_i^h at any point \mathbf{x} in the vicinity of σ_i^h , $i = 1, 2$ and is second order accurate;
- A gradient reconstruction operator G_i , which approximates the values of ∇u_i^h at any point \mathbf{x} in the vicinity of σ_i^h , $i = 1, 2$ and is second order accurate;
- A pair of discrete control spaces $L_{1,\sigma}^{2,h}$ and $L_{2,\sigma}^{2,h}$, defined on σ_1 and σ_2 , respectively, for the discretization of the virtual controls.

In [2] we defined R_i and G_i through polynomial extensions and chose $L_{i,\sigma}^{2,h}$ to be a piecewise constant space on σ_i^h . We retain the choice of virtual control spaces, but use instead the GMLS approximation (1) to define the R_i and G_i .

¹The choice of a unit normal on the interface is arbitrary. For example, one can choose the normal that coincides with the outer unit normal on σ considered as part of, e.g., $\partial\Omega_1$.

Specifically, given a point $\mathbf{x} \in \mathbb{R}^d$ we set

$$R_i u_i^h(\mathbf{x}) := \tau_{\mathbf{x}}^h(u_i^h),$$

where $\tau_{\mathbf{x}}^h$ is the GMLS approximation defined in (1). Likewise, we define

$$G_i u_i^h(\mathbf{x}) := (\tau_{\mathbf{x},1}^h(u_i^h), \dots, \tau_{\mathbf{x},d}^h(u_i^h)),$$

where $\tau_{\mathbf{x},i}^h$ is the GMLS approximation of the i th partial derivative defined in (2). These choices yield the following generalization of the objective (9) to non-coincident interfaces:

$$\begin{aligned} J_{\delta}^h(u_1^h, u_2^h, g_1^h, g_2^h) = & \frac{1}{2} \left[\int_{\sigma_1^h} (u_1^h - R_2 u_2^h)^2 dS + \int_{\sigma_2^h} (u_2^h - R_1 u_1^h)^2 dS \right. \\ & + \int_{\sigma_1^h} ((\kappa_1 \nabla u_1^h - \kappa_2 G_2 u_2^h) \cdot \mathbf{n}_1)^2 dS + \int_{\sigma_2^h} ((\kappa_1 G_1 u_1^h - \kappa_2 \nabla u_2^h) \cdot \mathbf{n}_2)^2 dS \\ & \left. + \left(\int_{\sigma_1^h} g_1^h dS + \int_{\sigma_2^h} g_2^h dS \right)^2 + \delta_1 \int_{\sigma_1^h} (g_1^h)^2 dS + \delta_2 \int_{\sigma_2^h} (g_2^h)^2 dS \right]. \end{aligned} \quad (10)$$

To summarize, the first two pairs of terms in (10) generalize the state misfit and the flux misfit terms in (9), and the fifth term controls the total flux misfit between the interfaces. The last two terms generalize the control penalties necessary for the well-posedness of the optimization problem. As a result, the discretization of (7) on non-coincident interfaces is given by the following problem:

$$\begin{aligned} & \text{minimize } J_{\delta}^h(u_1^h, u_2^h, g_1^h, g_2^h) \text{ over } H_{1,\Gamma}^h \times H_{2,\Gamma}^h \times L_{1,\sigma}^{2,h} \times L_{2,\sigma}^{2,h} \\ & \text{subject to a discretized form of the weak equations (8)}. \end{aligned} \quad (11)$$

4 NUMERICAL EXAMPLES

Patch test This example demonstrates the ability of the method to recover globally linear solutions. We set $u = 3x + 2y$ and define the Dirichlet boundary condition data and the right hand side by inserting this solution in (5).

For the patch test we use two different domain and mesh combinations and an S-curve interface parameterized by

$$\sigma = \{x = 1 + 0.1 \sin(1.5\pi t); y = t\}$$

In the first configuration (Figure 2a), Ω is the rectangle $[0, 2] \times [0, 1]$ and σ is an S-curve interface through the center of the computational domain. For this example we use relatively coarse subdomain meshes Ω_i^h having large and visible gaps and overlaps; see Fig. 3. The induced interface grids for this ‘‘coarse grid’’ example have element ratio 3 : 4.

In the second configuration (Figure 2b), Ω is the rectangle $[0.8, 1.2] \times [0, 1]$ and σ is again an S-curve interface through the center of the computational domain. The subdomain grids for this example are relatively finer but still have gaps and overlaps, albeit less

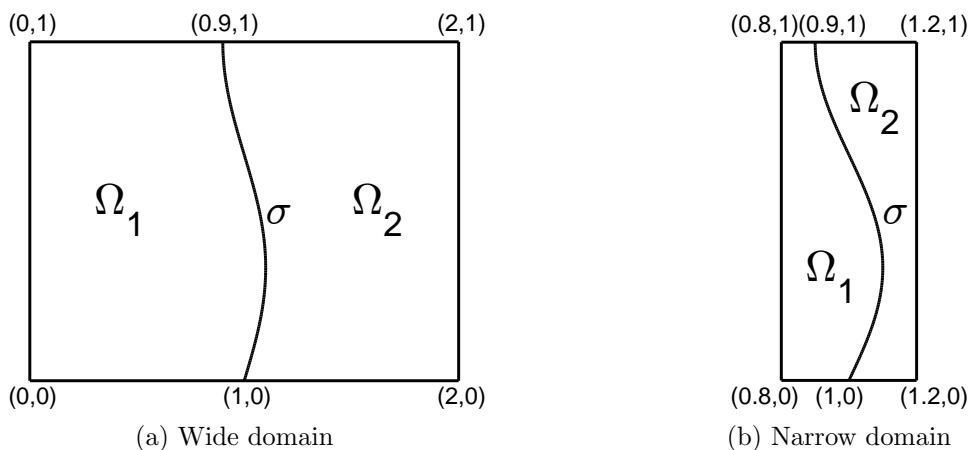


Figure 2: The first configuration (2a) is designed to accentuate the gaps and overlaps, while the second one (2b) aims to increase the surface area of the interface relative to the subdomain boundaries.

visible than in the first example. The induced interface grids for this “fine grid” example have element ratio 2 : 3. We solve (11) on both configurations with penalty terms set to 0. Using GMLS with order $m = 2$, the optimization formulation recovers the exact solution to machine precision in both cases; see Figures 3–4. Of note, using GMLS with order $m = 1$ in the optimization formulation also recovers the exact solution to machine precision.

Convergence rates To estimate the convergence rates of (11) we use the same manufactured solution and methodology as in [2]. Specifically, we set

$$u = x^2(y - 2)^3 \sin(2\pi x) - (x - 3)^3 \cos(2\pi x - y). \quad (12)$$

and define the right hand sides and Dirichlet boundary conditions by inserting (12) into (5). We solve (11) using several different combinations of subdomain grids to include a sufficiently representative range of interface element ratios. For each combination we start with an initial grid pair Ω_1^h and Ω_2^h having the desired element ratio on the interface. The initial pair is then refined successively six times while keeping the interface element ratio fixed. For all interface ratios in this study we set $\delta_1 = \delta_2 = 1e-10$ in the objective (10). Results in (5) confirm that both the H^1 -norm and L^2 -norm errors of the new formulation converge optimally.

5 CONCLUSIONS

We have extended the non-standard domain decomposition method of Gunzburger and Lee [7, 6] to spatially varying interface discretizations having gaps and overlaps. Our approach differs in that we have used a separate Neumann control on each subdomains’ interface and included additional terms to the cost functional to target the minimization of global flux mismatch as well as normal fluxes. We introduced the use of GMLS for

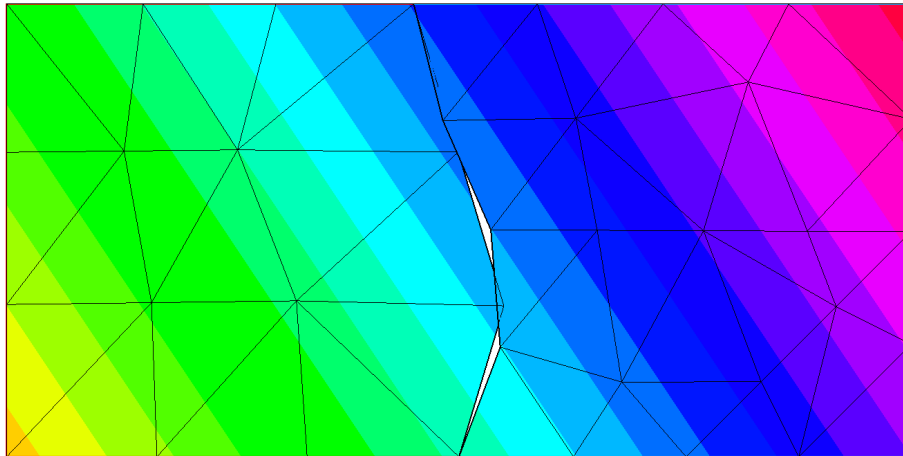


Figure 3: Patch test for an S-curve interface on coarse grids containing large gaps and overlaps. The interface grids σ_i^h have element ratio 3 : 4.

meshlessly evaluating and comparing function and gradient values between subdomains at quadrature points for terms in the objective of the minimization problem. This removed an accuracy bottleneck in the evaluation of the normal fluxes between subdomains while also avoiding the difficulties generally associated with mismatched and noncoincident interfaces including Taylor series extensions, projections or ray-tracing, or the construction of virtual interfaces. The method passes a linear patch test and converges optimally in both the H^1 -norm and L^2 -norm.

Acknowledgment

Sandia National Laboratories is a multimission laboratory managed and operated by National Technology and Engineering Solutions of Sandia, LLC., a wholly owned subsidiary of Honeywell International, Inc., for the U.S. Department of Energy’s National Nuclear Security Administration under contract DE-NA-0003525. SAND2018-6034 C.

The views expressed in the article do not necessarily represent the views of the U.S. Department of Energy or the United States Government.

This material is based upon work supported by the U.S. Department of Energy, Office of Science, Office of Advanced Scientific Computing Research and the Laboratory Directed Research and Development program at Sandia National Laboratories.

REFERENCES

- [1] P. Bochev and D. Day. A least-squares method for consistent mesh tying. *Int. J. Num. Anal. Model.*, 4:342–352, 2007.

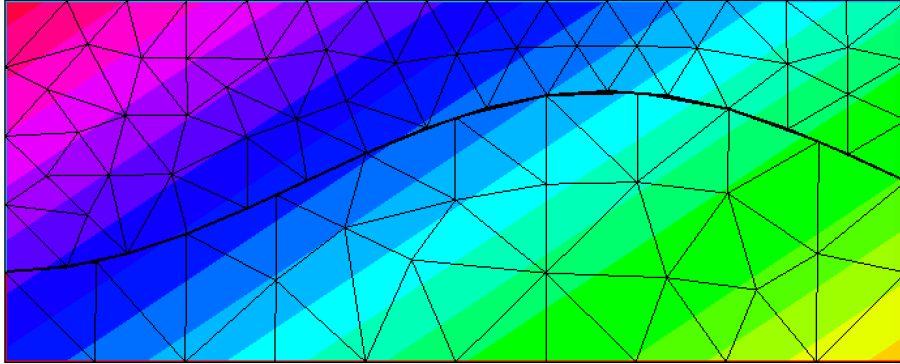


Figure 4: Patch test for an S-curve interface on fine grids containing small gaps and overlaps. The interface grids σ_i^h have element ratio 2 : 3. The figure is rotated 90 degrees counterclockwise.

- [2] Pavel Bochev, Paul Kuberry, and Kara Peterson. A virtual control coupling approach for problems with non-coincident discrete interfaces. In Ivan Lirkov, Svetozar Margenov, and Jerzy Waśniewski, editors, *Proceedings of the 11th International Conference, LSSC 2017, Sozopol, Bulgaria, June 5-9, 2017*, volume 10665 of *Lecture Notes in Computer Science*, pages 147–155. Springer Berlin Heidelberg, 2018.
- [3] G.F. Carey, S.S. Chow, and M.K. Seager. Approximate boundary-flux calculations. *Computer Methods in Applied Mechanics and Engineering*, 50(2):107 – 120, 1985.
- [4] C. R. Dohrmann, S. W. Key, and M. W. Heinstein. A method for connecting dissimilar finite element meshes in two dimensions. *Int. J. Numer. Meth. Eng.*, 48(5):655–678, 2000.
- [5] B. Flemisch, J.M. Melenk, and B.I. Wohlmuth. Mortar methods with curved interfaces. *Applied Numerical Mathematics*, 54(3–4):339 – 361, 2005. Selected papers from the 16th Chemnitz Finite Element Symposium 2003.
- [6] M. D. Gunzburger and H. K. Lee. An optimization-based domain decomposition method for the Navier-Stokes equations. *SIAM Journal on Numerical Analysis*, 37(5):pp. 1455–1480, 2000.
- [7] M. D. Gunzburger, J. S. Peterson, and H. Kwon. An optimization based domain decomposition method for partial differential equations. *Computers & Mathematics with Applications*, 37(10):77 – 93, 1999.

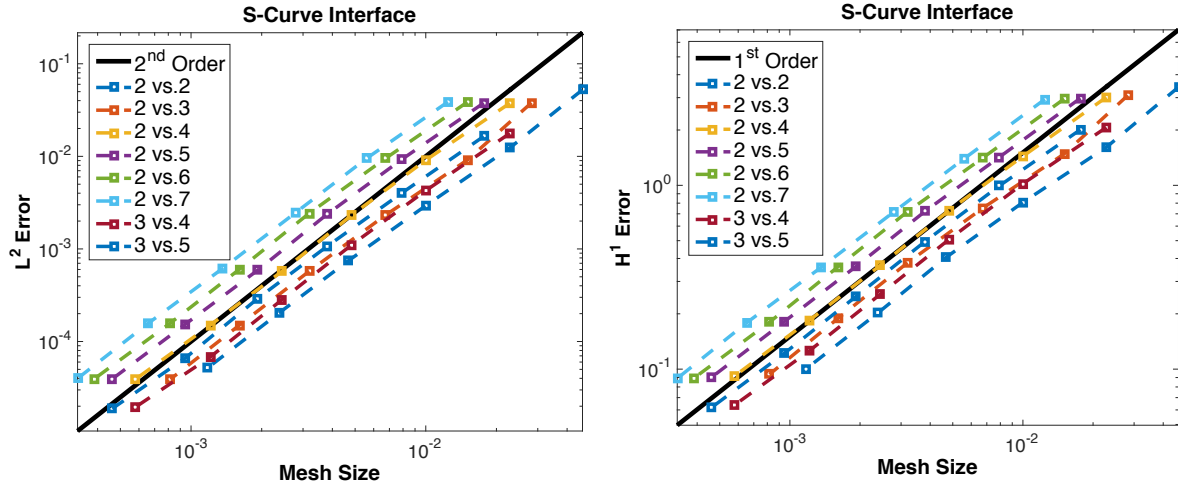


Figure 5: Convergence rates of (11) for interface grids having different element ratios. In each case the interface element ratio $|\sigma_1^h| : |\sigma_2^h|$ is preserved throughout the grid refinement process.

- [8] Thomas J.R. Hughes, Gerald Engel, Luca Mazzei, and Mats G. Larson. The continuous Galerkin method is locally conservative. *Journal of Computational Physics*, 163(2):467 – 488, 2000.
- [9] P. Kuberry, P. Bochev, and K. Peterson. An optimization-based approach for elliptic problems with interfaces. *SIAM Journal on Scientific Computing*, 39(5):S757–S781, 2017.
- [10] T. A. Laursen and M. W. Heinstein. Consistent mesh tying methods for topologically distinct discretized surfaces in non-linear solid mechanics. *International Journal for Numerical Methods in Engineering*, 57(9):1197–1242, 2003.
- [11] M.L. Parks, L. Romero, and P. Bochev. A novel lagrange-multiplier based method for consistent mesh tying. *Computer Methods in Applied Mechanics and Engineering*, 196(35–36):3335 – 3347, 2007.
- [12] Michael A. Puso. A 3d mortar method for solid mechanics. *International Journal for Numerical Methods in Engineering*, 59(3):315–336, 2004.
- [13] Holger Wendland. *Scattered data approximation*, volume 17. Cambridge university press, 2004.